

Free to move or trapped in your group: Mathematical modeling of information overload and coordination in crowded populations

A. Ciallella

E-mail: alessandro.ciallella@uniroma1.it

Dipartimento di Scienze di Base e Applicate per l'Ingegneria, Sapienza Università di Roma, via A. Scarpa 16, I-00161, Roma, Italy.

Emilio N.M. Cirillo

E-mail: emilio.cirillo@uniroma1.it

Dipartimento di Scienze di Base e Applicate per l'Ingegneria, Sapienza Università di Roma, via A. Scarpa 16, I-00161, Roma, Italy.

Petru L. Curşeu

E-mail: petrucurseu@psychology.ro

Department of Psychology Babes-Bolyai University, Republicii 37, Cluj-Napoca, 400015 Cluj, Romania.

Department of Organization, Open University of The Netherlands, Heerlen, The Netherlands.

Adrian Muntean

E-mail: adrian.muntean@kau.se

Department of Mathematics and Computer Science, Karlstad University, Sweden.

Abstract. We present¹ modeling strategies that describe the motion and interaction of groups of pedestrians in obscured spaces. We start off with an approach based on balance equations in terms of measures and then we exploit the descriptive power of a probabilistic cellular automaton model. Based on a variation of the simple symmetric random walk on the square lattice, we test the interplay between population size and an interpersonal attraction parameter for the evacuation of confined and darkened spaces. We argue that information overload and coordination costs associated with information processing in small groups are two key processes that influence the evacuation rate. Our results show that substantial computational resources are necessary to compensate for incomplete information – the more individuals in (information processing) groups the higher the exit rate for low population size. For simple social systems, it is likely that the individual representations are not redundant and large group sizes ensure that this non-redundant information is actually available to a substantial number of individuals. For complex social systems information redundancy makes information evaluation and transfer inefficient and, as such, group size becomes a

¹Preprint of an article submitted for consideration in Mathematical Models and Methods in Applied Sciences, 2018, World Scientific Publishing Company, www.worldscientific.com/worldscinet/m3as.

drawback rather than a benefit. The effect of group sizes on outgoing fluxes, evacuation times and wall effects are carefully studied with a Monte Carlo framework accounting also for the presence of an internal obstacle.

Keywords: phase coexistence, interface, compaction

AMS Subject Classification: 00A71, 80M31, 60J60, 92D25, 35L65

1. Introduction

1.1. *Towards modeling pedestrian group dynamics*

Social mechanics is a topic that has attracted the attention of researchers for more than one hundred years; see e.g. [25, 37]. A large variety of existing crowd dynamics models are able to describe the dynamics of pedestrians driven by a *desired velocity* towards clearly defined exits. But how can we possibly describe the motion of pedestrians when the exits are unknown or not clearly defined, or even worse, *what if the exits are not visible?*

This paper is inspired by a practical evacuation scenario. Some of the existing models are geared towards describing the dynamics of pedestrians with somehow given, prescribed or, at least, desired velocities or spatial fluxes towards an exit the location of which is, more or less, known to the pedestrians. Our contribution complements the existing work on crowd evacuation dynamics, see e.g. the papers [2, 3, 6, 33, 40, 41] and references cited therein.

We focus on modeling basic features that we assume to be influential for the motion of pedestrians in regions with reduced or no visibility. In our simulation studies, we focus on group size (social cluster size), population size, interaction with the walls of the confined space and the presence of an obstacle in the room as factors that might impact on information overload and coordination costs in social systems. In terms of output we focus both on the outgoing flux when the population size is constant and the evacuation time of the whole population in the confined space (under this condition, population size decreases constantly with the evacuation flux).

1.2. *A case study in group psychology. Aim of the paper.*

In a classic study in Social Psychology [39] the autokinetic effect is used to explore the formation of norms in social groups. The autokinetic effect is an optical illusion generated by a stationary light spot projected on a display in a darkened room, spot that appears to be moving [1]. In [39] participants are asked to estimate the amplitude of the movement of this light spot, first individually and then in dyads or groups of three. His observation was that although the individual estimates were substantially different, when group members could

hear each others answers, their estimations converged towards consensus on the amplitude of the movement. Moreover, when participants were first asked to estimate the amplitude of the movement in a group and then individually, the “norm” established in the group biased the individual estimations later on. Finally, it is a matter of convergence in time as the individual estimates did not converge after the first trial, in other words, group members needed time to synchronize their individual estimates [39]. This is one of the first empirical evidences that in ambiguous situations, people often use others as information resources to find clarity and come to accurate evaluations of environmental stimuli. In a similar fashion, in cases of fire emergency, in rooms filled with smoke, people are confronted with highly ambiguous stimuli and attempt to find clarity by interacting with others present in the same room (situation) [28].

The amount of information available to the population present in the room, increases with the population size as each member in the room may get access to a particular information that is otherwise inaccessible to the others in the room. In other words, the more people in the space to be evacuated, the higher the potential pool of information for the accurate evaluation of the situation. There are however limitations the information sharing possibilities in groups of varying sizes. As the experiment in [39], the individual estimates needed time to converge as during each exposure, participants slowly adjusted their individual estimation to the estimates of the other groups members, till eventually all estimates converged towards a group norm. These coordination constraints of individual actions in groups or communities have subsequently received substantial attention in the literature [32]. People are more likely to share information with the ones situated in their immediate presence, therefore information sharing and information integration attempts happen in smaller groups or clusters [19, 20, 26]. As the size of these small groups increases so does the coordination cost associated with information sharing and evaluation. The way in which people use each other as information resources in ambiguous situations is therefore constrained by at least two important socio-cognitive factors. The first one refers to the information pool available to a population exposed to highly ambiguous situations. As the population size increases, so does the potential information pool available in the system. The second one refers to the coordination constraints, as information sharing happens usually in smaller subgroups. As the size of the subgroup in which the information sharing takes place increases, so do the coordination costs associated with information sharing and information evaluation. An important problem therefore arises on how factors that might impose coordination constraints and generate information overload (the population size, the cluster size, interaction with walls and presence of obstacles) influence the identification of the exit and the successful room evacuation.

It is our aim to explore the interplay between the information overload and coordination costs as mechanisms that can explain the outgoing flux and the evacuation time of pedestrians. Information overload increases with the cluster or group size in which the information is shared and it decreases with the use of heuristics (e.g., identifying a wall that could lead to an exit), while coordination costs increase with the complexity of the system (described by the population size available in the room) and the presence of an obstacle in the room. We investigate the outgoing flux under various population sizes (for each simulated population size, population remains stable during the simulation) in order to capture the interplay between information overload and coordination costs. Moreover, we investigate the evacuation time in order to single out the role of group size (cluster size), interaction with the wall (as decision heuristic) and presence of an obstacle and further clarify the results of the outgoing flux.

1.3. Structure of the paper

The aim of the paper is stated in Subsection 1.2. In Section 2, we derive formally a balance equation for group-structured mass measures designed to describe the group formation (coagulation and fragmentation) similarly to a "thinking" flow of polymeric chains; see e.g. [16] for a nice brief introduction to models like Becker–Döring and Smoluchovski for polymeric flows. Agglomerating and binding monomers leads to our first "group concept". Moving to a totally different level of mathematical description, Section 3 contains a variation of a simple random walk on a square lattice to describe the interplay between the population size and interpersonal attraction parameters. The stochastic dynamics is biased by the presence of a threshold – our second attempt of a "group concept". The lattice model is getting to action in Section 4 and captures the effects of information overload and coordination in large disoriented populations. We conclude the paper with Section 5, where we summarize our main findings concerning our second concept of group of pedestrians.

2. A measure-theoretical modeling strategy

For modeling population dynamics, a natural mathematical tool is the concept of *mass* measure. This measure can flexibly represent either the distribution of individuals in a corridor, their number or their mass localized at a certain location as a function of possible features. Signed measures form a Banach space. The mass (finite) measures, which are responsible for handling the information pool, are a closed subset in this Banach space. Much of the theory of ordinary differential equations applies directly to dynamics in Banach spaces and therefore to measure-valued differential equations; see [30] for measure-valued equations offering descriptions of the evolution of an unstructured language or our recent work on

crowd dynamics [22, 23, 34], where the mass measures evolve in a bounded environment where boundary interactions are allowed. A nice account of measure-theoretical models in the context of crowd dynamics and traffic flows can be found in [18]. We need to mention already at this stage that the infinite dimensional geometry is often counter-intuitive and always requires a careful mathematical treatment (compare [8, 30]), not only what concerns solvability issues, but also from the perspective of a proper numerical approximation of the evolving measures [13]. We do not touch here any mathematical concerns around the obtained model. Instead we give a brief derivation of a structured-crowd model suitable for dynamics where visibility is obscured. The mathematical analysis needed to ensure the well-posedness of this model will be handled elsewhere. The result of our modeling exercise will turn to be a special case of a multi-feature continuity equation; cf. for instance [10, 11] or the related setting in [24]. We intend to provide here a general modeling framework for building “features”-based continuity-like equations for size-ordered interacting populations, which should be seen as an alternative of working with local balance laws using densities. The presentation recalls from [34]. In this context, the “location in the corridor” and the “group size” constitute the two “features”; we refer the reader to [21] for a related reading. The first feature is a continuous variable, while the second is a discrete variable. Their evolution is supposed to be continuous in time. In what follows, we derive a population-balance equation able to describe the evolution of pedestrian groups in obscured regions, relying on the same principles as in [11].

Fix $N \in \mathbb{N}$, let $\Omega \subset \mathbb{R}^2$ be the dark corridor (open, bounded with Lipschitz boundary), S - the observation time interval and $K_d := \{0, 1, 2, 3, \dots, N\}$ - the collection of all admissible group sizes. We say that a Y belongs to $K' \subseteq K$, if it belongs as part of some group with a size K . Furthermore, $\mathfrak{A}_\Omega := \mathfrak{B}^2(\Omega)$, $\mathfrak{A}_S := \mathfrak{B}^1(S)$ are the corresponding Borel σ -algebras with the corresponding Lebesgue-Borel measures $\lambda_x := \lambda^2$ and $\lambda_t := \lambda^1$, respectively; $\mathfrak{A}_{K_d} := \mathfrak{p}(K_d)$ is equipped with the counting measure $\lambda'_c(K) := |K'|$. We call $\lambda_{tx} := \lambda_t \otimes \lambda_x$ the *space-time measure* and set $\lambda_{txc} := \lambda_t \otimes \lambda_x \otimes \lambda_{c_j}$, $\mathfrak{A}_{\Omega K_d} := \mathfrak{A}_\Omega \otimes \mathfrak{A}_{K_d}$, $\mathfrak{A}_{S \Omega K_d} := \mathfrak{A}_S \otimes \mathfrak{A}_\Omega \otimes \mathfrak{A}_{K_d}$.

2.1. Balance of mass measures

Fix $t \in S$, let $\Omega' \in \mathfrak{A}_\Omega$, $K' \in \mathfrak{A}_{K_d}$, $S' \in \mathfrak{A}_S$, we introduce the target *amount* quantity

$$\begin{aligned} \mu_Y(t, \Omega' \times K') &:= \text{number of } Y's \text{ present in } \Omega' \\ &\text{at time } t \text{ and belonging to the group } K' \end{aligned} \tag{1}$$

together with two *inner production* quantities

$$\begin{aligned} \mu_{PY\pm}(S' \times \Omega' \times K') &:= \text{number of } Y's \text{ which are added} \\ &\text{to (subtracted from) } \Omega' \times K' \text{ during } S' \text{ and} \end{aligned} \tag{2}$$

$$\mu_{PY} = \mu_{PY+} - \mu_{PY-}.$$

Note that these numbers might be non-integers, which is not *per se* realistic. Furthermore, group size changes are allowed and we state that a group size 1 exist, which is virtually incorrect. From a sociologic perspective, one is an individual/agent, two is a dyad and from 3 onward we can speak about groups. Consequently, when we describe the change from the size $N=2$ to $N-1=1$, the dyad becomes an individual. An increase from 1 to 2 is a transition from individual to dyad in a location, while a change from 2 to 3 is a transition from a dyad to a group.

Given the nature of the problems we are dealing with, we postulate the following key properties our mass measures are supposed to fulfil:

(P1) For all $K' \in \mathfrak{A}_{K_d}$, $\Omega' \in \mathfrak{A}_\Omega$ and $t \in S$: $\mu_Y(t, \cdot \times K')$ and $\mu_Y(t, \Omega' \times \cdot)$ are measures on their respective σ -algebras \mathfrak{A}_Ω and \mathfrak{A}_{K_d} , respectively.

(P2) $\mu_{PY\pm}(S' \times \Omega' \times \cdot)$, $\mu_{PY\pm}(S' \times \cdot \times K')$ and $\mu_{PY\pm}(\cdot \times \Omega' \times K')$ are measures on their respective σ -algebras.

Now, we are in the position to formulate the balance principle:

$$\begin{aligned} \mu_Y(t+h, \Omega' \times K') - \mu_Y(t, \Omega' \times K') &= \mu_{PY}(S' \times \Omega' \times K') \\ \text{for all } t, t+h \in S, \Omega' \times K' \in \mathfrak{A}_\Omega \times \mathfrak{A}_{K_d}, S' &:= (t, t+h]. \end{aligned} \quad (3)$$

Addition to $\Omega' \times K'$, modeled by μ_{PY+} , can happen by addition *inside* of $\Omega' \times K'$ as well as by fluxes *into* $\Omega' \times K'$. A similar remark applies to subtraction and μ_{PY-} . This gives rise to the assumption that μ_{PY+} is actually the sum of an interior production part, μ_{PY+}^{int} , and a flux part, μ_{PY+}^{flux} , i.e. an accumulation of interior and boundary productions. We proceed similarly with μ_{PY-} . Finally, we obtain the representation of the net productions

$$\begin{aligned} \mu_{PY}^{int} &:= \mu_{PY+}^{int} - \mu_{PY-}^{int} \text{ and } \mu_{PY}^{flux} := \mu_{PY+}^{flux} - \mu_{PY-}^{flux}, \\ \mu_{PY} &= \mu_{PY+}^{int} + \mu_{PY+}^{flux} = (\mu_{PY+}^{int} - \mu_{PY-}^{int}) + (\mu_{PY+}^{flux} - \mu_{PY-}^{flux}). \end{aligned} \quad (4)$$

We extend $\mu_Y(t, \cdot \times \cdot)$ and $\mu_{PY\pm}(\cdot \times \cdot \times \cdot)$ by the usual procedure to measures $\bar{\mu}_Y = \mu_Y(t, \cdot)$ and $\bar{\mu}_{PY\pm} = \mu_{PY\pm}(\cdot)$ on the product algebras $\mathfrak{A}_\Omega \otimes \mathfrak{A}_{K_d}$ and $\mathfrak{A}_S \otimes \mathfrak{A}_\Omega \otimes \mathfrak{A}_{K_d}$, respectively. Note that the quantities in (P1) and (P2) and the extensions are finite.

The following postulate prevents mass accumulation on sets of measure zero. It reads as

(P3) $\bar{\mu}_Y(t, \cdot) \ll \lambda_{xc}$ (absolutely continuous).

Therefore, for all $t \in S$ there exist integrable Radon–Nikodym densities $u(t, \cdot) = \frac{d\bar{\mu}_Y(t, \cdot)}{d\lambda_{xc}}$, i.e.

$$\bar{\mu}_Y(t, Q') = \int_{Q'} u(t, (x, i)) d\lambda_{xc} \text{ for all } Q' \in \mathfrak{A}_{\Omega K}. \quad (5)$$

The absolute–continuity assumption

$$(P4) \quad \bar{\mu}_{PY}^{int} \ll \lambda_{txc}$$

excludes the presence of Y 's on sets of λ_{txc_1} -measure zero. Furthermore, it assures the existence of the Radon–Nikodym density

$$f_{PY}^{int} := \frac{d\bar{\mu}_{PY}}{d\lambda_{txc}} \in L_{loc}^1(S \times \Omega \times K_d, \mathfrak{A}_{S\Omega K_d}, \lambda_{txc}). \quad (6)$$

To get a reasonable idea for a representation of the flux measure, we consider the special case $Q' = \Omega' \times K'$ with, say, $K' = \{a, a+1, \dots, b\} \in \mathfrak{p}(K_d)$. The "surface"

$$\mathfrak{F} := \Omega' \times \{a\} \cup \Omega' \times \{b\} \cup \partial\Omega' \times K'$$

is the location of any interaction with the outside of Q' . There are two locations on \mathfrak{F} to enter or to leave Q' from the outside – one via $\mathfrak{F}_1 := \Omega' \times \{a\} \cup \Omega' \times \{b\}$, the other one through $\mathfrak{F}_2 := \partial\Omega' \times K'$.

The unit-outward normal field $\mathbf{n} = \mathbf{n}(x, \kappa)$ on \mathfrak{F} can be split into two orthogonal components, $\mathbf{n} = \mathbf{n}_x + \mathbf{n}_\kappa$, $\mathbf{n}_x = (n_x, 0)$, $\mathbf{n}_\kappa = (0, n_\kappa)$, respectively. It is $n_\kappa(x, a) = -1$, $n_\kappa(x, b) = +1$ and $n_x = n_x(x, \kappa)$ is the a.e. existing outward normal on $\partial\Omega$. Borrowing from the theory of Cauchy interactions, cf. [38], e.g., we postulate the following:

(P5) Assume, for all $t \in S$, the existence of two *flux vector fields*

$$\begin{aligned} j_x(t, \cdot) &: \Omega \times K_d \rightarrow \mathbb{R}^2 \\ j_\kappa &: \Omega \times K_d \rightarrow \mathbb{R} \end{aligned}$$

inter-linked via

$$\bar{\mu}_{PY}^{flux} := \bar{\mu}_{PY_x}^{flux} + \bar{\mu}_{PY_\kappa}^{flux},$$

where

$$\begin{aligned} \bar{\mu}_{PY_x}^{flux}(S' \times \Omega' \times K') &:= \int_{S'} \int_{\mathfrak{F}_2} -j_x(\tau, x, i) \cdot n_x(x, i) d\sigma_x d\lambda_c d\tau \\ &\text{and} \\ \bar{\mu}_{PY_\kappa}^{flux}(S' \times \Omega' \times K') &:= \int_{S'} \int_{\Omega'} -j_\kappa(\tau, x, b) n_\kappa(x, b) \\ &\quad - j_\kappa(\tau, x, a) n_\kappa(x, a) dx d\tau. \end{aligned} \quad (7)$$

In (7), σ_x - is the 1D-curve length measure. The term $\bar{\mu}_{PY_x}^{flux}(S' \times \Omega' \times K')$ calculates the net gain/loss of the Y 's in Ω' belonging to one of the size groups from K' due to physical motion from/to the outside of Ω' into/out of Ω' . Note that the quantity $\bar{\mu}_{PY_\kappa}^{flux}(S' \times \Omega' \times \{i\})$ calculates the net gain/loss of the Y 's in Ω' belonging to the size group labelled by i . There

is no interaction with groups of size $\kappa > N$ or $\kappa < 0$ since these sizes are considered here as unadmissible. In this case, we require

$$j_\kappa(t, x, 0) = j_\kappa(t, x, N) = 0 \quad \text{for all } t \in S, x \in \Omega. \quad (8)$$

Introducing the *discrete partial derivative* by

$$\partial_i^d j_\kappa(t, x, i) := j_\kappa(t, x, i+1) - j_\kappa(t, x, i), \quad i \in K$$

and assuming u , f_{PY}^{int} , $\text{div}_x j_x$ and $\partial_\kappa^d j_\kappa$ to be sufficiently regular, we obtain

$$\begin{aligned} \bar{\mu}_{PY}^{flux}(S' \times Q') &= \int_{S'} \int_{Q'} -\text{div}_x(j_x(\tau, x, i)) d\lambda_c dx d\tau \\ &\quad + \int_{S'} \int_{Q'} -\partial_i^d j_\kappa(t, x, i) d\tau dx d\lambda_c. \end{aligned}$$

Combining (3) – (7), Fubini's theorem, and division by $h > 0$, imply

$$\begin{aligned} &\int_{Q'} \frac{1}{h} (u(t+h, x, i) - u(t, x, i)) dx d\kappa \\ &= \int_{Q'} \frac{1}{h} \int_t^{t+h} (f_{PY}^{int}(\tau, x, i) - (\text{div}_x j_x(\tau, x, i) + \partial_i^d j_\kappa(\tau, x, i))) d\tau dx d\lambda_c. \end{aligned}$$

Under appropriate smoothness conditions on u , f_{PY}^{int} , j_x and j_κ we obtain in the limit $h \rightarrow 0$ (the classical continuity equation with a slightly different interpretation of the entries)

$$\frac{\partial u}{\partial t}(t, x, i) + (\text{div}_x j_x + \partial_i^d j_\kappa(t, x, i)) = f_{PY}^{int}(t, x, i). \quad (9)$$

The existence of the underlying measures is a matter that will be investigated at a later stage, in a different context.

As in [34], we can point out a direct connection with a suitable Becker–Döring–like model for colloidal interactions (cf. e.g. [16] and references cited therein), which mimics well the dynamics of groups of individuals in dark. To do so, one has to specify the flux vectors j_x and j_κ as well as the production term f_{PY}^{int} .

For $i = 1, \dots, N$, we set

$$\begin{aligned} J_x(t, x, i) &= -D_i(u_i(t, x)) \text{grad}_x(u_i(t, x)), \\ f_{PY}^{int}(t, x, i) &= \begin{cases} \sum_{i=1}^N \alpha_i u_i - \sum_{i=1}^N \beta_i u_i u_1 & \text{if } i = 1, \\ \beta_{i-1} u_{i-1} u_1 - \beta_i u_i u_1 & \text{if } i \in \{2, \dots, N-1\}, \\ \beta_N u_{N-1} u_1 & \text{if } i = N, \end{cases} \end{aligned}$$

The discrete derivative $j_\kappa(t, x, i)$ corresponds to

$$\begin{aligned} j_\kappa(t, x, i) &= -\alpha_i u_i(t, x), \quad i = 1, 2, \dots, N-1, \\ j_\kappa(t, x, 0) &= j_\kappa(t, x, N) = 0. \end{aligned}$$

Specifying $j_x(t, x, i)$ as some sort of a degenerating diffusion flux in the manner above means: Individual groups of size i recognize whether a group of the same size is in their immediate neighborhood and they tend to avoid moving into the direction of such groups. Employing a Fickian law seems to be the simplest way to model this. The degeneration in the flux appears especially if the dynamics is thought to take place in domains with obstacles, where the percolation of the "thinking" fluid locally clogs when obstacles are too close from each other.

The production term f_{PY}^{int} models merging interactions between groups of size $i \in K$ and "groups" of size $i = 1$: If an individual meets a group of size $i < N$, then it might happen, that this single merges with the group. This turns the group into a group of size $i + 1$ and leads to a "gain" for groups of size $i + 1$ (modeled by $+\beta_i u_i u_1$) and a loss for groups of size i (modeled by $-\beta_i u_i u_1$). In any such joining situation the group with $i = 1$ loses members (modeled by $-\sum_{i=2}^N \beta_i u_i u_1$). Note, that this model allows only for direct interaction between groups of size i with groups of size 1. Using a Smoluchowski dynamics instead would relax this constraint [16]. The α -terms model the group fragmentation effect: It might happen, that an individual leaves a group of size $i \geq 2$. This leads to a loss for the groups of size i (modeled by $-\alpha_i u_i$) as well as to a gain for the groups of size $i - 1$ and a gain for the groups with $i = 1$ (modeled by $\sum_{i=2}^N \alpha_i u_i$). In simple crowd simulations [34], the coefficients $\alpha_i, \beta_i \geq 0$ and $D_i > 0$ can be assumed to be constant. It is interesting to note that the fragmentation terms express a flux rather than a volume source or sink. In the same way as aging can be seen as a flux ("people change their age group by aging with (speed 1)"), Y 's change their size group by "degradation" of their group. Nevertheless, for a fixed size choice i , the expressions $\alpha_i u_i$ and $\alpha_{i-1} u_{i-1}$ still remain "volume sources" and "volume sinks", respectively.

The mathematical analysis of this model can be approached for instance by adapting the techniques from [9] to our setting combined with arguments specific to handling porous media-like equations. However, we do not expand on this matter here and prefer instead to propose a lattice model not only to describe at the microscopic level the motion of the crowd in dark, but also to quantify the information overload and coordination in crowded populations.

3. A lattice-based modelling strategy

3.1. The lattice model

Our model was introduced in [14, 15] by adapting ideas introduced in [4] to study the ionic currents in cell membranes and further developed in [5]. For an introduction to stochastic processes, we refer the reader e.g. to [35].

To describe our model, we start off with the construction of the lattice. Let $e_1 = (1, 0)$ and $e_2 = (0, 1)$ denote the coordinate vectors in \mathbb{R}^2 . Let $\Lambda \subset \mathbb{Z}^2$ be a finite square with odd side length L . We refer to this as the *corridor*. Each element x of Λ will be called a *cell* or *site*. The external boundary of the corridor is made of four segments made of L cells each; the point at the center of one of these four sides is called *exit*.

Let N be positive integer denoting the (total) *number of individuals* inside the corridor Λ . We consider the state space $X = \{0, \dots, N\}^\Lambda$. For any state $n \in X$, we denote by $n(x)$ be the *number of individuals* at cell x .

We define a Markov chain n_t on the finite state space X with discrete time $t = 0, 1, \dots$. The parameters of the process are the integer $T \geq 0$ called *threshold*, $W \geq 0$ called *wall stickiness*, and the real number $R \in [0, 1]$ called the *rest parameter*. We finally define the function $S : \mathbb{N} \rightarrow \mathbb{N}$ such that

$$S(k) = 1 \text{ if } k > T \quad \text{and} \quad S(k) = k + 1 \text{ if } k \leq T$$

for any $k \in \mathbb{N}$. Note that for $k = 0$ we have $S(0) = 1$.

At each time t , the N individuals move simultaneously within the corridor according to the following rule: for any cell x situated in the interior of the corridor Λ , and all y nearest neighbor of x , with $n \in X$, we define the weights $w(x, x) = RS(n(x))$ and $w(x, y) = S(n(y))$. Also, we obtain the associated probabilities $p(x, x)$ and $p(x, y)$ by dividing the weight by the normalization

$$w(x, x) + \sum_{i=1}^2 w(x, x + e_i) + \sum_{i=1}^2 w(x, x - e_i).$$

Let now x be in one of the four corners of the corridor Λ , and take y as one of the two nearest neighbors of x inside Λ . For $n \in X$, we define the weights $w(x, x) = RS(n(x)) + 2W$ and $w(x, y) = S(n(y)) + W$ and the associated probabilities $p(x, x)$ and $p(x, y)$ obtained by dividing the weight by the suitable² normalization. In this case we are introducing the additional term W that is mimicking the stickiness of the wall. That is this parameter takes

²To get a probability, we divide the weights by the sum of the involved weights: It is about 3 terms if the site lies in a corner of the corridor, 4 terms if it is close to a border, and then 5 terms for a pedestrian located in the core.

into account the possibility that people prefer to move nearby the wall in condition of lack of visibility.

It is worth stressing, here, that T is not a threshold in $n(x)$, the number of individuals per cell, but a threshold in the probability that such a cell is likely to be occupied or not.

For $x \in \Lambda$ neighboring the boundary (but neither in the corners, nor neighboring the exit), y one of the two nearest neighbor of x inside Λ and neighboring the boundary, z the nearest neighbor of x in the interior of Λ , and $n \in X$, we define the weights $w(x, x) = RS(n(x)) + W$, $w(x, y) = S(n(y)) + W$, and $w(x, z) = S(n(z))$. The associated probabilities $p(x, x)$, $p(x, y)$, and $p(x, z)$ are obtained by dividing the weight by the suitable normalization.

Finally, we define the weights if x is the site in Λ neighboring the exit. We propose two different choices mimicking two different situations. If the exit is clearly identifiable, particles in the neighboring cell exit with probability 1. This exit modelling will be called *sure exit* case. If the exit is not clearly identifiable, we although assume it is the most likely site to jump to and we treat it as if it were occupied by the threshold number of pedestrians. More precisely, in this case, called the *threshold exit case*, if y is one of the two nearest neighbor of x inside Λ and neighboring the boundary and z is the nearest neighbor of x in the interior of Λ , we define the weights $w(x, x) = RS(n(x))$, $w(x, y) = S(n(y)) + W$, $w(x, z) = S(n(z))$, and $w(x, \text{exit}) = T + 1$, for the configuration $n \in X$. The associated probabilities $p(x, x)$, $p(x, y)$, $p(x, z)$, and $p(x, \text{exit})$ are obtained by dividing the weight by the suitable normalization.

At time zero, the individuals are randomly located inside the corridor. The dynamics is then defined as follows: at each time t , the position of all the individuals on each cell is updated according to the probabilities defined above. If one of the individuals jumps on the exit cell a new individual is put on the cell of Λ neighboring $\partial\Lambda$ and opposite to the exit site.

3.2. Social groups in search for information

As we argued before, information sharing happens in smaller social groups. In our lattice model, group size is modeled as an attraction parameter that stimulates agents to move in particular locations of the lattice in which a predefined number of agents is already present. We will define the thresholds for this attraction parameters using existing research on human groups formation. In an overview of how social cognition emerges in groups [12] it is argued that the dyad (a group of two) is the smallest social entity in which microcoordination processes take place. In a similar vein, in [31] it is argued that dyads are specific forms of social aggregates in which coordination costs are minimal as these aggregates consist of just a single relationship, are simpler than larger groups, in other words, dyads are social aggregates in which information pool and coordination costs are low. Following the categorization of social aggregates based on size, in [12] the author further distinguishes between work/family groups, demes and macrodemes. The small groups (of size 5) that in evolutionary terms

resemble small families, are social aggregates in which division of labor can be observed and coordination constraints increase as they are formed of several dyadic relations [31]. The so-called demes (larger groups of size 30 or bands) are the first organizational forms in which economic activities and transactions are undertaken and therefore involve higher coordination. Finally, the macrodemes (larger communities of size 300) are social aggregates that can deal with highly complex environments (including survival under limited resource availability) [12]. In other words, the macrodemes are the social aggregates in which both potential information pool and coordination costs are high. Although, as argued in [12] the group sizes used to distinguish between these social aggregates are not exact estimates, we decided to follow this categorization in defining the small group in which potential information sharing takes place. In the simulation, these various small group sizes described above are represented by the number of agents per site that maximizes the probability of an agent to jump on that site. For this reason, we will use the parameter $T = 0, 2, 5, 30$, and 300.

We further on consider the interaction with the walls of the room as a decision heuristic used to oversimplify the complexity of the available information. Decision-makers often use heuristics to speed-up their decision processes and as such they select a small amount of information they process. In particular, the wall could signal the likely location of an exit, as an exit is always tied to a wall. We therefore introduce this heuristic as a way of mitigating the information overload, especially in large populations. Finally, we model the effect an obstacle located either at the center of the room, or close to the exit has on the outgoing flux and evacuation time. An obstacle increases the coordination costs as it may interfere with the cluster formation and the effective movement towards the exit.

4. The lattice model in action – simulation of social groups

We explore numerically the effect of groups sizes (threshold) on the outgoing flux, on the interaction with the walls and eventual fixed obstacles, as well as on the evacuation time.

4.1. The outgoing flux

In this section, the main quantity of interest is the outgoing flux [4,5,14,15], i.e., the average number of individuals exiting the corridor per unit of time. Recall that the unit of time is the time in which all the individuals are moved. In our simulations, we consider as corridor Λ a square lattice with side $L = 101$ and $W = 0$ (if not mentioned otherwise).

Fig. 1 and Fig. 2 show the outgoing flux plotted as a function of the number of pedestrians N in the case in which $R = 0$ for the two different exit rules considered, while in Fig. 3 the same for $R = 1$ is plotted. In Fig. 1 and Fig. 2, on the right side, it is represented the zoom of the picture on the left side of Fig. 1 and Fig. 2, respectively, for small population size (below 3000).

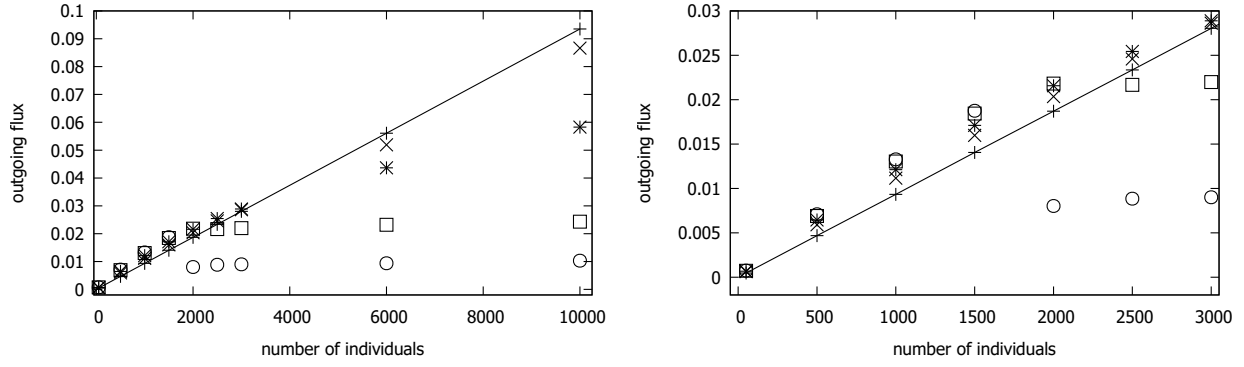


Figure 1: **Outgoing flux for $R = 0$.** On the left: outgoing flux for $R = 0$ and *threshold exit rule*. On the right: zoom for the outgoing flux for $R = 0$ case and $N \leq 3000$. The symbols $+$, \times , $*$, the square and the circle refer respectively to the cases $T = 0, 2, 5, 30, 300$.

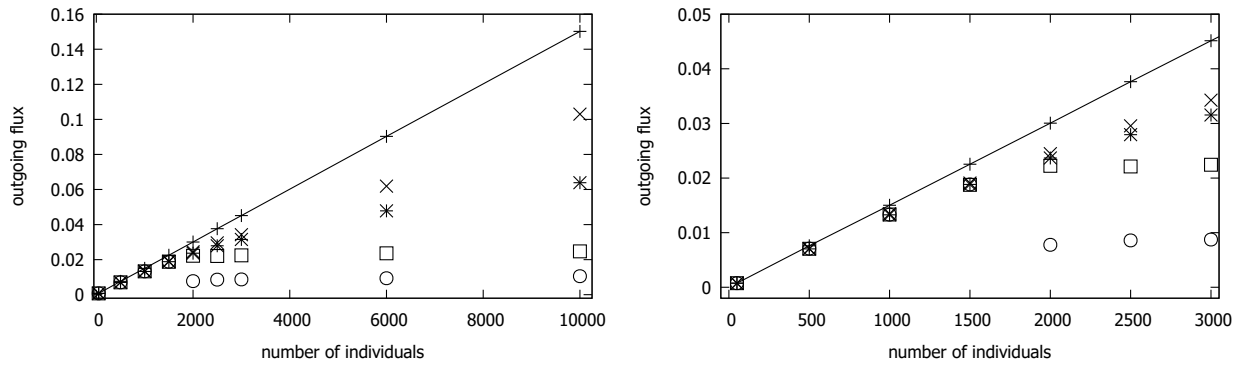


Figure 2: **Outgoing flux for $R = 0$.** On the left: outgoing flux for $R = 0$ and *sure exit rule*. On the right: zoom for the outgoing flux for $R = 0$ case and $N \leq 3000$. The symbols $+$, \times , $*$, the square and the circle refer respectively to the cases $T = 0, 2, 5, 30, 300$.

For a large number of pedestrians the cooperation effects incorporated by the use of the threshold T are not as efficient as a Brownian (egoistic) walk. In the case of the threshold exit rule, for a small number of particles (say, below $N = 3000$), we observe that the presence of the threshold in our lattice dynamics accelerates the particles motion leading to fluxes higher than the ones obtained for the Brownian motion. Furthermore, switching from the rest probability $R = 1$ to the rest probability $R = 0$ enhances the threshold influence on the evacuation flux. This effect is new and non-intuitive.

As one expects, the choice of the *sure exit* favors the outgoing flow. Indeed, in this case the individuals in front of the exit go always out of Λ at the first next update of their position, while in the other case they can remain in Λ with positive probability. This is neatly proven by the data for the case of $T = 0, 2$, but it is not so evident for larger thresholds. In Fig. 4

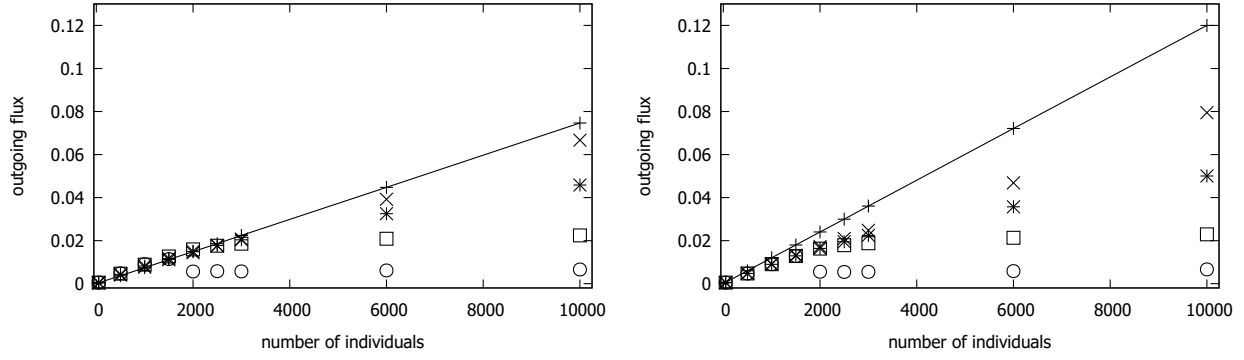


Figure 3: **Outgoing flux for $R = 1$.** On the left the plot of the threshold exit case while on the right the plot of the sure exit case. The symbols $+$, \times , $*$, the square and the circle refer respectively to the cases $T = 0, 2, 5, 30, 300$.

data relating to the two exit rules are compared for $T = 5, 30, 300$. Black and grey symbols are closer and closer when T is increased, this means that the difference between the two cases vanishes when T grows.

This effect can be explained as the consequence of our choice for the probability to exit for a particle facing the exit in the *threshold exit* case. Indeed, for small values of T , such as $T = 0, 2$, the weight $T + 1$ we assign to the exit site is comparable to the weight associated with the other neighboring sites, so that the particles often remain in the system instead of jumping to the exit. This is not the case for larger values of T , since the weight associated with the exit site is likely to be significantly larger than the one assigned to the other neighboring sites. Hence, in this case, the system behaves similarly to the sure exit case.

This remark explains the effect observed in Fig. 1 and stressed in the zoom. For small values of N , the average outgoing exit flux has an increment in the case of large threshold with respect to the independent random walk case ($T = 0$), if we consider the threshold exit rule. This is due to the fact that in a regime of small number of individuals, it is really unlikely to have many individuals on the nearest neighbors of the sites closest to the exit, so the weight of the exit site is clearly much larger than the other nearest neighbors. Thus, the probability to jump out is significantly bigger for large T than in the case of small values of the threshold.

This phenomenon is observed only in the case of small density of individuals, and it is obviously not present for the sure exit rule. If the particle density is increased, then the interaction among individuals plays a much more important role in the dynamics, influencing crucially the behavior of the overall flux and the overshoot finally disappears.

The simulation results show some very interesting patterns for the interplay between

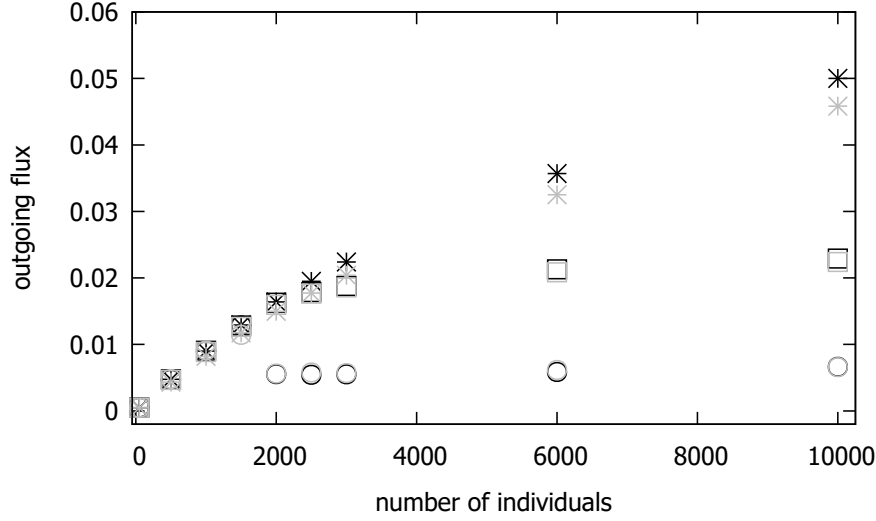


Figure 4: **Averaged outgoing flux vs. number of pedestrians.** We show a comparison of the simulation results for $T = 5$ (*), 30 (squares), 300 (circles), in the case of *sure exit* (in black), and in the case of *threshold exit* (in gray) for $R = 1$. Note that gray and black circles and squares are overlapping.

potential information pool and coordination costs on the rate of exit per unit of time. As the system complexity (illustrated by the population size) increases from low to average it seems that the higher potential information pool associated with larger subgroups pays off and the rate of exit increases above the base rate ($T = 0$). However, as the complexity of the system further increases (above population size 2000) the coordination costs (generated by the fact that very large clusters are actually formed) outweigh the benefits of higher potential information pool. The rate of exit levels off for $T = 300$ (at around population size 2000), for $T = 30$ at around 2500, for $T = 5$ at around 6000, while for $T = 2$ the exit rate is only slightly lower than the base rate at the population size 10000.

A plausible interpretation of these results is that as environmental complexity increases from average to high, the coordination costs become the most important factor that drives the exit rate per unit of time. For simpler systems, a high number of cognizers organized in groups seem to be essential in getting as many people out of the room as possible, while for highly complex systems, dyads seem to suffice.

In other words, in systems with a substantial number of agents (higher than 2000), for $T = 300$, very large groups can easily form and as they are built, coordination costs block effective information sharing in these groups and the large clusters become stuck in a lengthy decision process. Large groups (300 members) once formed, start information sharing and try to reach a decision on actions to be taken. However, integrating the vast amount of

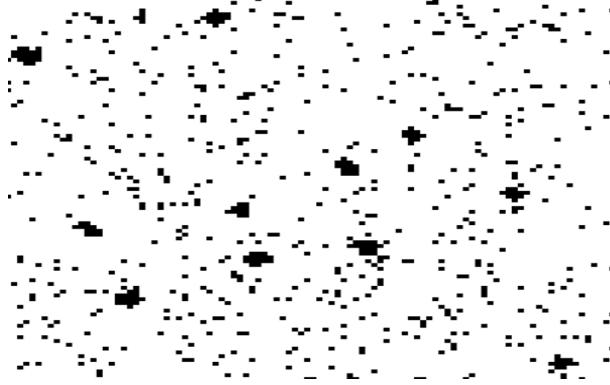


Figure 5: **Typical configuration.** Typical configuration of the system at large time in the case $R = 1$, $T = 300$, $L = 101$, and $N = 10000$. White and black points denote, respectively, empty and occupied sites of the lattice.

information brought in by the large number of agents takes a substantial amount on time and effort.

Next to the coordination constraints, members in large groups tend to exert less effort towards the collective goal, therefore social loafing increases with groups size [27]. It is therefore likely that agents will spend a substantial amount of “effortless” time in such large clusters that will ultimately prevent them from exiting as indicated in Fig. 5 that depicts the cluster formation behavior for $N = 10000$ and $T = 300$.

4.2. *The interaction with the wall*

We study the dependence of the dynamics on the possible choice of the parameter W , which we refer to as *wall stickiness*. We introduce this parameter to take into account the possibility that the pedestrian may have the tendency to move close to the wall as main personal reaction to the lack of visibility and a heuristic for finding an exit.

We expect that the choice of a positive value for the parameter W can improve the outward flux. This intuition follows from the fact that the number of sites neighboring the boundary are of order of $\mathcal{O}(L)$, while the total number of sites is of order of $\mathcal{O}(L^2)$. So the choice of the parameter $W > 0$ (illustrative of a decision heuristic “A wall indicates the location of an exit”) helps reducing the random walk on a number of sites of lower order and the individuals will find the exit earlier.

On the other hand, we expect that the agents localization close to the wall may favor the formation of clusters of particles as all agents may use the same heuristic. In our view, the increased coordination costs associated with this agglomerations close to the walls could be a mechanism leading to the slowing down of the evacuation.

Our simulations show that the leading effect is the increase of the flux rate. In Fig. 6, we show the effect of the wall interaction on the outgoing flux. We plot the measured average outgoing flux for different values of $W \geq 0$. In the figure, to have a readable picture, we show the cases $T = 0$ in the left panel, and the cases $T = 5$ and $T = 300$ in the right panel, but the increasing effect is present for any value of the threshold. We use grey tones to distinguish the values assumed by $W = 0, 1, 3, 5, 10$, using lighter tone when W is larger. For any fixed value of the threshold T , the flux increases monotonically with respect to W . The increment is bigger when the clustering effect is not so strong, hence for small values of T .

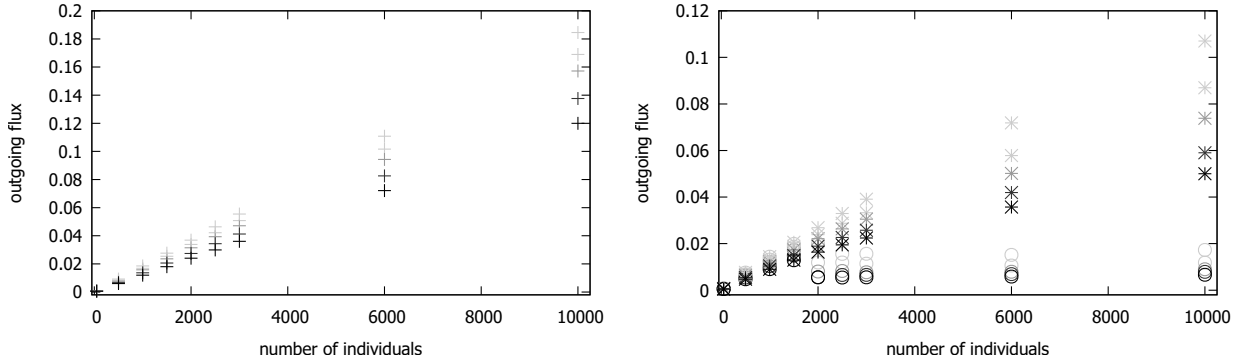


Figure 6: **Averaged outgoing flux vs. number of pedestrians.** Simulations with $L = 101$, $R = 1$, and, from the darkest to the lower grey, $W = 0, 1, 3, 5, 10$. On the left: plot of the average outgoing flux for $T = 0$ (+). On the right: plot of the average outgoing flux for $T = 5$ (*) and $T = 300$ (circles).

It is interesting to observe that even if the measured value of the flux increases when W grows, for any fixed value of W the plot of the average flux as function of N has the same behavior of the one resulting in the case $W = 0$. To illustrate this observation, we show in Fig. 3 a plot analogous to the one we made for $W = 0$. The qualitative behavior of the outgoing flux as a function of N does not change for $W > 0$. We see in Fig. 7 illustrating the case $W = 3$ that with both the sure exit and threshold exit rules the plots are similar to those in Fig. 3.

We also notice that even in this case, as observed earlier for $W = 0$, the clustering regime starts for $T = 300$ when the number of individuals grows up to 2000. If a small number of particles ($N \leq 1500$) is involved in the dynamics, then the measured outgoing fluxes for any fixed value of the parameter W are really close. As a consequence, the measured flux does not depend on T for these values of N .

We argued that the interaction with the wall is a plausible decision heuristic that could

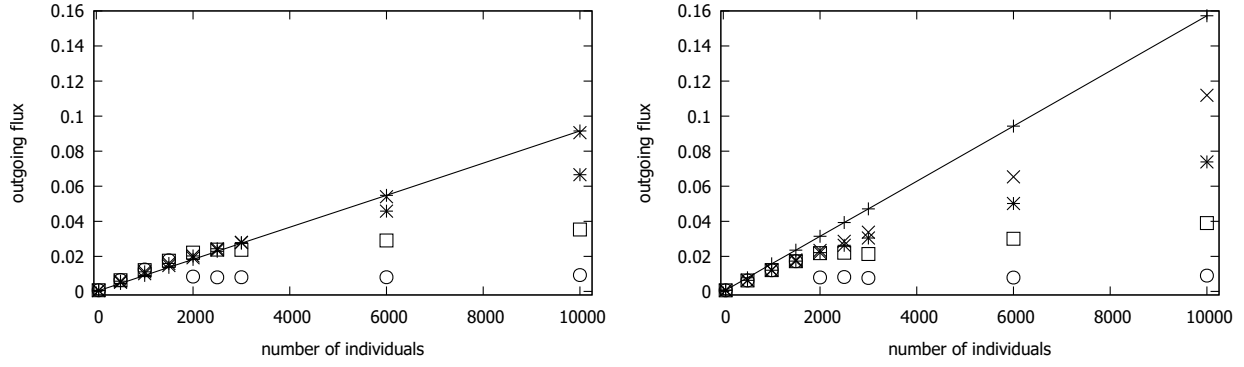


Figure 7: **Averaged outgoing flux vs. number of pedestrians.** The symbols $+$, \times , $*$, the squares and the circles represent respectively the cases $T = 0, 2, 5, 30, 300$, with $L = 101$, with $W = 3$, and $R = 1$. On the left we show the simulation results for the choice of the *threshold exit*, on the right the data refer to the *sure exit* rule.

decrease the information overload associated with large population sizes. In line with this expectation, for low population size, the variation in interaction with the wall makes no substantial difference in the outgoing flux, supporting the observation that in simple environments, heuristics are not particularly useful. As information overload increases for population sizes larger than 2000, the small groups ($T=5$) seem to benefit more from the use of this decision heuristic than the large groups ($T=300$). However, as mentioned earlier, the outgoing flux seems to increase in all group sizes when interaction with the walls increase. So in general, this decision heuristic seems to be an effective way of coping with information overload, yet it cannot completely override the coordination costs associated with large groups.

4.3. The role of the obstacle

We consider now the presence of a square obstacle inside the corridor. The obstacle is expected to increase the coordination costs because it may wrongly signal an exit, and reduce freedom to move in the room. We vary two indices related to the obstacle, namely its size and its location as parameters that can represent the increase in coordination costs associated with the obstacle. When the object is small or located in the center its impact on coordination costs is expected to be lower than when the object is large and located close to the exit. The obstacle is represented by a number of sites in the corridor that are not accessible to the agents. Note that the sites in the corridor neighboring the obstacle but accessible to the individuals will be considered as boundary sites, i.e., the agents might prefer to move close to this internal boundary due to the possible wall stickiness W .

We expect that the obstacle can influence the resulting outgoing flux, because of excluded

volume, in two different ways. On the one hand it can make easier or harder for a particle to find the exit depending on its position, for instance making more difficult to reach a region far from or close to the exit. On the other the presence of an obstacle can favor the clustering formation and influence the region in which the cluster is formed.

We notice in our simulation that if the obstacle is sufficiently small it does not visibly affect the flux, so we consider now the case of a squared obstacle with side 41. In Fig. 8 we show the behavior of the flux if it is present this squared obstacle with side 41 with center in the center of the corridor.

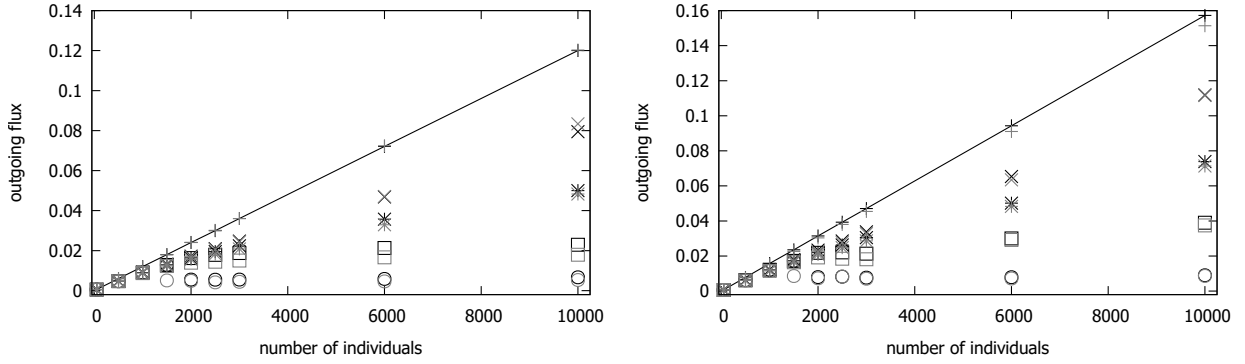


Figure 8: **Averaged outgoing flux vs. number of pedestrians.** The symbols $+$, \times , $*$, the squares and the circles represent respectively the cases $T = 0, 2, 5, 30, 300$, with $L = 101$, $R = 1$, *sure exit* rule and a squared obstacle with side 41 placed in the lattice with center in $(51, 51)$. The grey symbols represent the case of presence of the obstacle, while the black symbols refer to the empty lattice. On the left we show the simulation results for $W = 0$, on the right the data refer to $W = 3$.

Small values of the threshold lead to small variations in the average exit flux. We can see this trend for $T = 0, 2$, and 5 . It is instead interesting to note the clustering induced by the obstacle for large values of T . The flux drop for $T = 300$ happens for $N = 1500$ both if $W = 0$ and if $W = 3$. We recall that, in the absence of the obstacle, we observe this flux drop for $T = 300$ for the first time around $N = 2000$ (see Fig. 1–2). For $T = 30$ the flux in the case $W = 0$ is reduced by the cluster formation (see the squares in Fig. 8, in the left panel, the grey symbols are always below the black).

We find a strong asymmetry in the positioning of the obstacle with respect to the center of the corridor. Let us first consider the same 41×41 obstacle, but we position it to be closer to the exit than to the opposite side of the lattice. In Fig. 9, we show the data for the square with center in $(71, 51)$. We find out that this obstacle close to the exit results in a loss in the outgoing flux (in figure we find the grey symbols always below the blacks, both if

$W = 0$ and $W = 3$). It is interesting to notice that now the clustering effect does not appear for smaller N compared to the case of the corridor without obstacle.

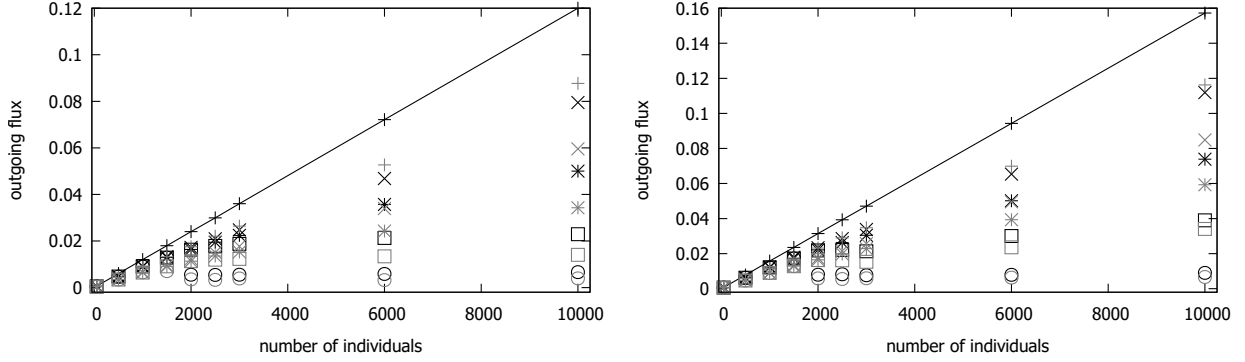


Figure 9: **Averaged outgoing flux vs. number of pedestrians.** As in figure 8, with a squared obstacle with side 41 and center in $(71, 51)$.

As expected, we observed in this case that an obstacle close to the exit cannot increase the average flux. Consider now the square with center in $(31, 51)$. We see in Fig. 10 that, for this particular choice of geometry, the outgoing flux increases if the threshold is not too large ($T \leq 5$ in the plot). On the contrary, if the threshold is large, $T \geq 30$ in the figure, we can observe that the clustering regime is reached earlier than in the empty corridor case. Indeed, there is a loss in the outgoing flux for $T = 30$ and $W = 0$, and the clustering appears at $N = 1000$ for the parameters $T = 300$ and $W = 0$, while at $N = 1500$ for $T = 300$ and $W = 3$.

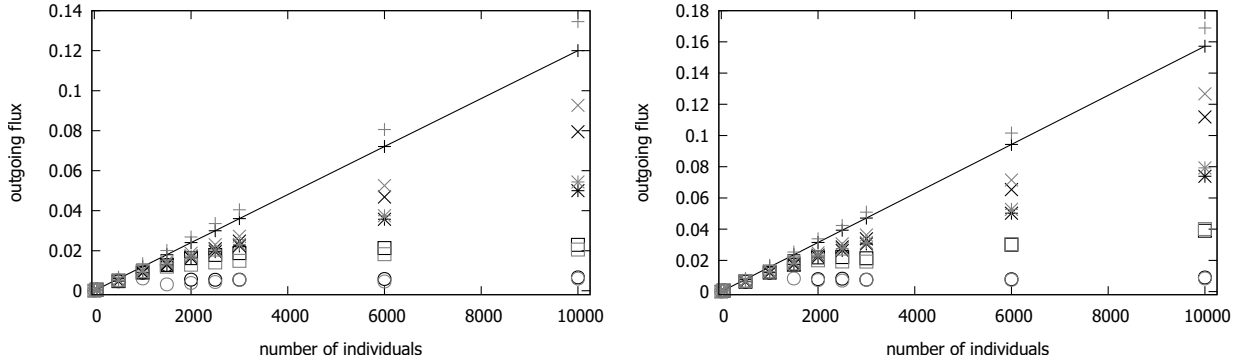


Figure 10: **Averaged outgoing flux vs. number of pedestrians.** As in Fig. 8, with a squared obstacle with side 41 and center in $(31, 51)$.

Summarizing, we find a strong dependence on the position of the obstacle. If the obstacle is closer to the exit than to the opposite side, the flux decreases. On the contrary,

if the obstacle is close to the entrance and far from the exit, the flux increases for small T . Interestingly, if the threshold is large, an obstacle close to the entrance favors the formation of clusters.

Our interpretation of the results is the following: The obstacle, placed close to the exit, makes more difficult to reach the region on its right side where there the exit location is, and, it produces a decrease in the outgoing flux with respect to the empty lattice case.

An obstacle close to the other side makes difficult for a particle to reach again the region on the left side of the obstacle once it is on the right side. It keeps the particles to spend longer time in the region with the exit, favorizing the exit. However, since the obstacle reduces the free region close to the entrance point, it makes more likely the formation of a big stable cluster in that region. This may produce a decrease in the flux, when coordination constraints are significant, namely if the group size is sufficiently big and the population size is sufficiently large. In other words we find that an obstacle adds coordination constraints when is large in size, situated next to the exit and the population and group sizes are large. We find that the outgoing flux is impaired in overcrowded spaces, with large clusters formed and in which a large obstacle is present next to the exit. Efficient information integration in small-sized groups can overcome the coordination constraints added by an obstacle, especially if this is not located next to the exit. This novel insights lends support for our initial interpretation that smaller groups are more effective information processing units and cope easier with the coordination problems.

4.4. *Evacuation time*

We are interested in evaluating the evacuation time, i.e., the average time needed to let all the individuals leave the corridor.

We consider the following experiment: We dispose N pedestrians randomly in the corridor and let the dynamics start accordingly with the description of the model in Sect. 3.1, but we do not consider any new individual entering in the corridor. We observe the time needed until the last pedestrian will exit the corridor. The average time measured repeating this experiment will be called *evacuation time*.

The results discussed concerning the outgoing flux allow us to argue which behaviors would be observed for the evacuation time. Note that since the number of agents is decreasing during the evolution of the system, it will be more difficult to enter in a clustering regime (i.e., it is necessary a larger number of particles to reach it) and the coordination constraints in the system are likely to be lower especially for small group and population sizes. Building on the results on the effect of an obstacle on the outgoing flux, we expect to find analogously that the evacuation time is smaller when the corridor is empty and if an obstacle is far from

the exit. On the contrary, the closer an obstacle is to the exit, the longer it will take for all particles to exit the room.

We plot in Fig. 11 the evacuation time as a function of the number of individuals N , for $W = 0$, and values for T from 0 to 300. The geometry is the corridor without the obstacle.

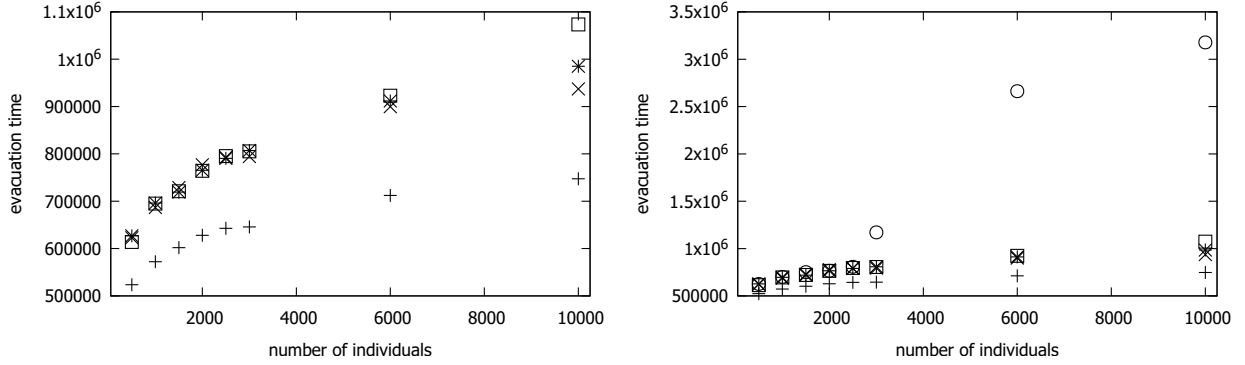


Figure 11: **Averaged evacuation time vs. number of pedestrians.** The symbols +, \times , $*$, the squares and the circles represent respectively the cases $T = 0, 2, 5, 30, 300$, with $L = 101$, $W = 0$, $R = 1$, sure exit and no obstacles in the corridor. On the left we excluded the results for $T = 300$ to have a more readable figure, on the right we have the same picture added of the data for $T = 300$.

We observe that the evacuation time is monotone with respect to T for a fixed N if N is large, while is essentially not depending on $T > 0$ if N is small. The independent random walk for $T = 0$ guarantees the minimum evacuation time. Note also that the system reaches the clustering regime only for large values of the threshold T and for large N , for $N \geq 3000$ when $T = 300$ in the plot. Note that in this clustering regime there is a clear growth in the evacuation time.

The presence of the obstacle leads to expected effects on the evacuation time. As discussed in the previous section, we consider a large squared obstacle with side 41 and we position it to be either in the left half of the corridor or in the right half. We report in Fig. 12–13 the average evacuation time calculated for the empty corridor (black symbols) and for the presence of the obstacle of side 41 with center in $(31, 51)$ as in Fig. 10 (grey symbols). We consider the cases of no influence by the wall on the dynamic ($W = 0$) in Fig. 12 and the case of positive W in Fig. 13. The presence of the obstacle in the left half of the corridor, far from the exit, produces a decrease in the evacuation time in most of the considered data. It is interesting to note that for $W = 0$ and $T = 300$ (Fig. 12, right picture) the clustering effect starts for a smaller number of agents with respect to the empty corridor case, so for $T = 300$ and N between 2500 and 3000 the evacuation time is longer if the obstacle is present. Once

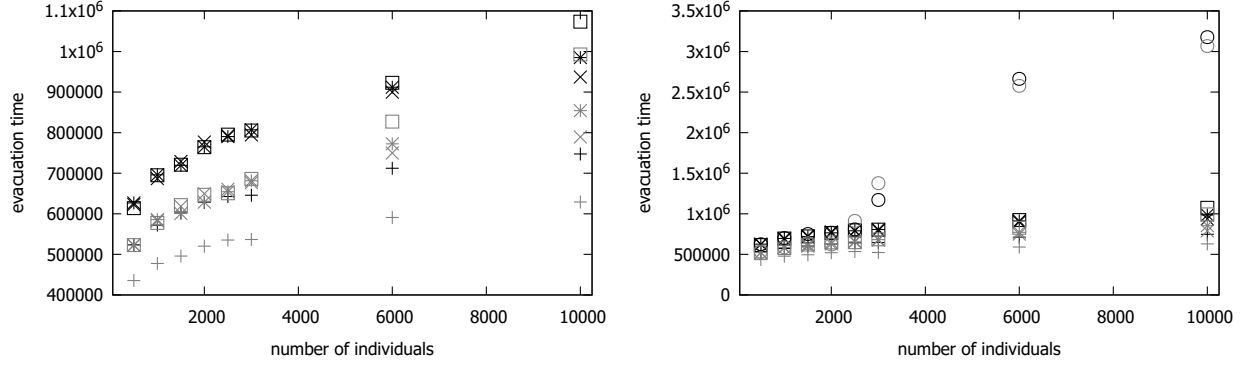


Figure 12: **Averaged evacuation time vs. number of pedestrians.** The symbols $+$, \times , $*$, the squares and the circles represent respectively the cases $T = 0, 2, 5, 30, 300$, with $L = 101$, $W = 0$, $R = 1$, sure exit and a squared obstacle with side 41 and center in $(31, 51)$ in the corridor. The gray symbols represent the case of presence of the obstacle, while the black symbols refer to the empty lattice. On the left we excluded the results for $T = 300$ to have a more readable figure, on the right we have the same picture added of the data for $T = 300$.

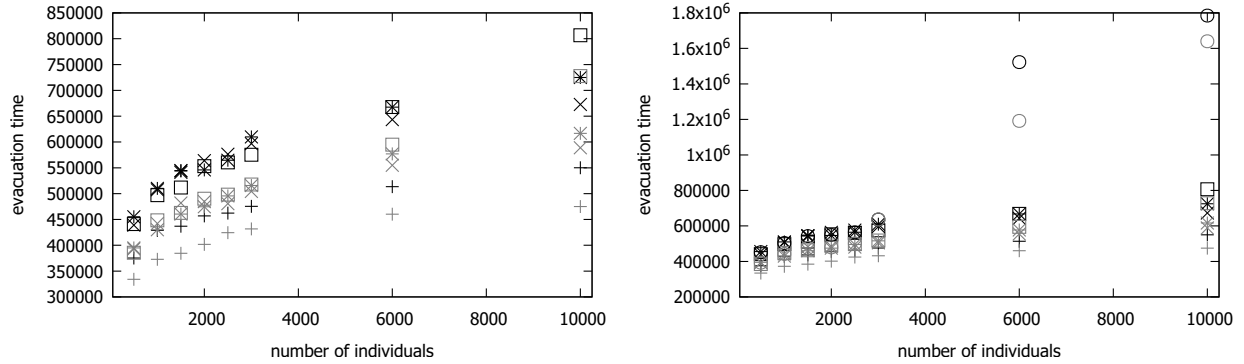


Figure 13: **Averaged evacuation time vs. number of pedestrians.** As in Fig. 12 with $W = 3$.

the clustering regime is reached in both cases (large N), the obstacle yields again a shorter evacuation time.

In Fig. 14 we consider the presence of the same square obstacle in the right half of the corridor, closer to the exit. We compare the evacuation time in presence of this obstacle (gray symbols) and in absence of obstacles (black symbols). The center of the obstacle is now put in $(71, 51)$. As in the case of the evaluation of the outgoing flux we find this positioning to be unfavorable, i.e., it produces an increment in the evacuation time, both if $W = 0$ (left picture) and if $W = 3$ (right picture).

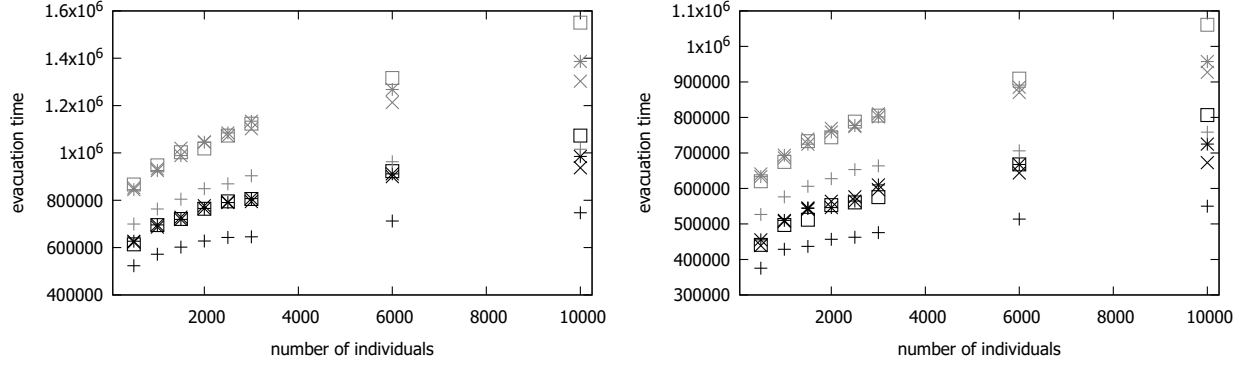


Figure 14: **Averaged evacuation time vs. number of pedestrians.** The symbols $+$, \times , $*$ and the squares represent respectively the cases $T = 0, 2, 5, 30$, with $L = 101$, $R = 1$, sure exit and a squared obstacle with side 41 and center in $(71, 51)$ in the corridor. The gray symbols represent the case of presence of the obstacle, while the black symbols refer to the empty lattice. On the left we show the simulation results for $W = 0$, on the right the data refer to $W = 3$.

4.5. Discussion

As population size increases the likelihood of information complexity in the general system increases as well (a large number of individuals develop partial representations about an otherwise ambiguous environment), therefore the benefit of higher information pool in subgroups decreases in importance. In other words, groups of minimum size take advantage of low coordination costs and information redundancy in the general population in order to speed up evacuation. Therefore, for large population size, the information complexity of the whole system overrules the benefit of information sharing in small groups varying in size. These results are somehow similar with the simulation results reported by [17] showing that as the population size increases the number of informed individual needed to direct the flock decreases. For $R=0$ individuals are required to move while for $R=1$ the probability of individual movement imposed is lower. This constraint increases the likelihood of exit especially for subgroups of smaller size (dyads and groups of five). This result supports the argument that informational complexity available in the system propagates better if individuals are asked to change positions as compared with the situation in which they can preserve their position on the lattice. Therefore, for systems of high information complexity (i.e., large population size) the probability of movement increases the rate of exit for smaller groups more than for large groups. As individuals (are forced to) move they acquire information from others in the room and, consequently, they will develop faster accurate interpretations concerning the availability of exit routes. To conclude, increasing the probability that in-

dividuals will freely move in the room, increases the rate of exit, by fostering information exchange that will ultimately accentuate the overriding effect of whole systems information complexity over the small group information pool.

As we argued before, the informational complexity of the whole system generates a blockage for large groups. Large groups seem to be effective in integrating informational inputs in simpler rather than highly complex systems as indicated in Fig. 1 where the exit rate increases with T for population size under 1500. Under situations of informational scarcity, group size seems to be a prerequisite for effective evacuation simply because the population size does not allow the formation of very large groups. In highly complex systems, the coordination costs (it becomes too difficult to find ways in which individual actions are to be synchronized in the whole system) and information processing costs (there are too many different information inputs that need to be integrated and the cluster is basically clogged) become unsurmountable for extremely large groups ($T = 300$).

Dyads, requiring minimal coordination costs, are better able to integrate effectively the (otherwise diverse) individual information inputs generated by frequent interactions especially imposed under $R = 0$. The monotonic flattening of the exit rate graph for $T = 30, 5, 2$ (rather than a sudden decrease as for $T = 300$) shows that these small group configurations are actually the only viable (social) information processing units in highly complex social environments. If large groups are more effective information integrators in rather simple social environments marked by ambiguity, dyads become the most effective information integrators in ambiguous environments with high social complexity.

The results for the interaction with the walls resemble following some sort of decision heuristic (it is a higher chance of finding an exit in a wall than in other locations in the room) so following this heuristic circumvents the added value of larger groups sharing information in a particular location.

The results show that effective information processing in small groups overrides coordination costs only in small populations. Moreover, the use of decision heuristics (i.e., presence of a wall) seems to increase the efficient information processing especially in small groups formed in dense population spaces. Coordination costs seem to be clearly disadvantageous especially when the group size is very large. In other words information integration in very large groups will not override the coordination costs associated with group size. Moreover, additional coordination constraints, like obstacles situated next to the exit, will further increase the negative effects of coordination costs both on outgoing flux as well as the evacuation time.

5. Conclusions

This study started from the observation that in ambiguous situations people use others to validate the information they have and this process plays an important role in situations in which a crowd needs to evacuate a darkened space. We claimed that the information pool (how many members are exposed to stimuli) and groups computational resources (how many members actually evaluate informational inputs) are two key factors influencing the speed of evacuation.

Our simulation results suggest that few information sources require large clusters, in other words, scarcity of information requires large computational resources. Moreover, we show that many information sources require small groups for effective evacuations as information redundancy requires little computational resources. As information resources become redundant, due to the high coordination costs in large groups and social loafing processes large groups become actually clogged by redundant information and evacuation rate decreases substantially.

A direct policy implication of our results is to stimulate the formation of very small group sizes (up to 5 members) when people are trapped in confined and darkened spaces, as this seems to foster both the outgoing flux as well as the evacuation time for the whole population.

Acknowledgements

ENMC and AM thank ICMS (TU/e, Eindhoven, The Netherlands) for the kind hospitality and for financial support. PLC was supported by a grant of the Romanian National Authority for Scientific Research, CNCS – UEFISCDI, project number PN-III-P4-ID-ERC-2016-0008. The funders had no role in study design, data collection and analysis, decision to publish, or preparation of the manuscript.

References

- [1] H.F. Adams, Autokinetic sensations. *Psychological Monographs* **14**, 1–45 (1912).
- [2] J.P. Agnelli, F. Colasuonno, D. Knopoff, A kinetic theory approach to the dynamics of crowd evacuation from bounded domains. *Mathematical Models and Methods in Applied Sciences* **25**, 109–129 (2015).
- [3] G. Albi, M. Bongini, E. Cristiani, D. Kalise, Invisible control of self-organizing agents leaving unknown environments. *SIAM J. Appl. Math.* **76**, 1683–1710 (2016).

- [4] D. Andreucci, D. Bellaveglia, E.N.M. Cirillo, S. Marconi, Monte Carlo study of gating and selection in potassium channels. *Physical Review E* **84**, 021920 (2011).
- [5] D. Andreucci, D. Bellaveglia, E.N.M. Cirillo, A model for enhanced and selective transport through biological membranes with alternating pores. *Mathematical Biosciences* **257**, 42–49 (2014).
- [6] N. Bellomo, D. Clarke, L. Gibelli, P. Townsend, B.J. Vreugdenhil, Human behaviours in evacuation crowd dynamics: From modelling to “big data” toward crisis management. *Physics of Life Reviews* **18** 1–21 (2016).
- [7] N. Bellomo, B. Piccoli, A. Tosin, Modeling crowd dynamics from a complex system viewpoint. *Math. Models Methods Appl. Sci.* **22**, Suppl. 02, 1230004, (2012).
- [8] V. I. Bogachev, Measure Theory, vol. 1, Springer Verlag, Berlin, 2007.
- [9] V. I. Bogachev, G. da Prato, M. Röckner, On parabolic equations for measures. *Comm. Partial Diff. Eq.* **33**, 1-3, 397–418 (2008).
- [10] M. Böhm, Lecture Notes in Mathematical Modeling. Fachbereich Mathematik und Informatik, Universität Bremen, Germany, 2012.
- [11] M. Böhm, M. Höpker, A note on modelling with measures: Two-features balance equations. *Math. Biosc. Engineering* **12**, 2, 279–290 (2015).
- [12] L.R. Caporael, The evolution of truly social cognition: The core configurations model. *Personality and Social Psychology Review* **1**, 276–298 (1997).
- [13] J. A. Carrillo, P. Gwiazda, A. Ulikowska, Splitting-particle methods for structured population models: Convergence and applications. *Mathematical Models and Methods in Applied Sciences* **24**, 11, 2171–2197 (2014).
- [14] E.N.M. Cirillo, A. Muntean, Can cooperation slow down emergency evacuations? *Comptes Rendus Macanique* **340**, 626–628 (2012).
- [15] E.N.M. Cirillo, A. Muntean, Dynamics of pedestrians in regions with no visibility – a lattice model without exclusion. *Physica A* **392**, 3578–3588 (2013).
- [16] J.-F. Collet, Some modelling issues in the theory of fragmentation-coagulation systems. *Commun. Math. Sci.* **2**, 1, 35–54 (2004).

- [17] I.D. Couzin, J. Krause, N.R. Franks, S.A. Levin, Effective leadership and decision-making in animal groups on the move. *Nature* **433**, 513–516 (2005).
- [18] E. Cristiani, B. Piccoli, A. Tosin, Multiscale Modeling of Pedestrian Dynamics, Series in Modeling, Simulation and Applications, vol. 12, Springer International Publishing, 2014.
- [19] P.L. Curşeu, R. Schalk, I. Wessel, How do virtual teams process information? A literature review and implications for management. *Journal of Managerial Psychology* **23**, 628–652 (2008).
- [20] P.L. Curşeu, O. Krehel, J.H. Evers, A. Muntean, Cognitive distance, absorptive capacity and group rationality: A simulation study. *PloS One* **9**, e109359 (2014).
- [21] O. Diekmann, M. Gyllenberg, J. A. Metz, H. R. Thieme, On the formulation and analysis of general deterministic structured population models I. Linear Theory. *Journal of Mathematical Biology* **36**, 4, 349–388 (1998).
- [22] J. H. M. Evers, S. C. Hille, A. Muntean, Mild solutions to a measure-valued mass evolution problem with flux boundary conditions. *Journal of Differential Equations* **259**, 3, 1068–1097 (2015).
- [23] J. H. M. Evers, S. C. Hille, A. Muntean, Mild solutions to a measure-valued mass evolution problem with flux boundary conditions. *SIAM J. Math. Anal.* **48**, 3, 1929–1953 (2016).
- [24] M. Gyllenberg Mathematical aspects of physiologically structured populations: the contributions of J. A. J. Metz, *Journal of Biological Dynamics*, **1**,1, 3–44 (2007).
- [25] S. Haret, Mécanique sociale. Gauthier-Villars, Paris, 1910.
- [26] V. Hinsz, Teams as technology: Strengths, weaknesses, and trade-offs in cognitive task performance. *Team Performance Management* **21**, 218–230 (2015).
- [27] A.G. Ingham, G. Levinger, J. Graves, V. Peckham, The Ringelmann effect: Studies of group size and group performance. *Journal of Experimental Social Psychology* **10**, 371–384 (1974).
- [28] B. Latané, J.M. Darley, Group inhibition of bystander intervention in emergencies. *Journal of Personality and Social Psychology* **10**, 215 (1968).
- [29] G. Le Bon, La psychologie des foules. The Echo Library, Middlesex, 2008.

- [30] W. Mitchener, Mean-field and measure-valued differential equation models for language variation and change in a spatially distributed population. *SIAM J. Math. Anal.* **42**, 5, 1899–1933 (2010).
- [31] R.L. Moreland, Are dyads really groups? *Small Group Research* **41**, 251–267 (2010).
- [32] J.S. Mueller, Why individuals in larger teams perform worse. *Organizational Behavior and Human Decision Processes* **117**, 111–124 (2012).
- [33] F. Müller, O. Wohak, A. Schadschneider, Study of influence of groups on evacuation dynamics using a cellular automaton model. *Transportation Research Procedia* **2**, 168–176 (2014).
- [34] A. Muntean, E.N.M. Cirillo, O. Krehel, M. Böhm, Pedestrians moving in the dark: Balancing measures and playing games on lattices. In *Collective Dynamics from Bacteria to Crowds: An Excursion Through Modeling, Analysis and Simulation*, CISM Lectures **553**, Springer, 2014.
- [35] G. A. Pavliotis, Stochastic Processes and Applications: Diffusion Processes, the Fokker-Planck and Langevin Equations. Texts in Applied Mathematics, vol. 60, Springer Verlag, Berlin, 2014.
- [36] B. Piccoli, A. Tosin, Time-evolving measures and macroscopic modeling of pedestrian flow. *Arch. Ration. Mech. Anal.* **199**, 3, 707–738 (2011).
- [37] A. Portuondo y Barceló, Apuntes sobre Mecánica Social. Establecimiento Topográfico Editorial, Madrid, 1912.
- [38] F. Schuricht, A new mathematical foundation for contact interactions in continuum physics. *Arch. Ration. Mech. Anal.* **433**, 169–196 (2007).
- [39] M. Sherif, A study of some social factors in perception. *Archives of Psychology*. **27**(187), 23–46 (1935).
- [40] J.-H. Wang, J.-H. Sun. Principal aspects regarding to the emergency evacuation of large-scale crowds: A brief review of literatures until 2010. *Procedia Engineering* **71**, 1–6 (2014).
- [41] S. Xue, B. Jia, R. Jiang, J. Shan, Pedestrian evacuation in view and hearing limited condition: The impact of communication and memory. *Physics Letters A* **380**, 3029–3035 (2016).